Fine Pointing Control for Free-Space Optical Communication

Angel A. Portillo, Gerardo G. Ortiz , Caroline Racho
Jet Propulsion Laboratory
California Institute of Technology
Pasadena, CA

ABSTRACT

Free-Space Optical Communications requires precise, stable laser pointing to maintain optimal operating conditions. This paper also describes the software and hardware implementation of Fine Pointing Control based on the Optical Communications Demonstrator architecture. The implementation is designed to facilitate system identification of the Fast Steering Mirror mechanism. Models are derived from laboratory testing of two fine steering mirrors that are integrated into the fine tracking loop. Digital controllers are then designed to close the tracking loop using optical feedback. Results of the Fine Pointing Control performance show an improvement of 20% in the jitter rejection bandwidth over previous experiments. A discussion of the computer delay and limited processing bandwidth in this particular implementation are included.

Keywords: Free-Space Optical Communications, Fine Pointing Control

1.0 Introduction

This paper describes improvements made to the existing implementation of the JPL patented Optical Communications Demonstrator Acquisition and Fine Tracking. A laboratory test bed has been developed for the purpose of analyzing, implementing, and testing a high bandwidth, precision pointing and tracking system for free-space optical communications. The test bed system allows for the implementation of Acquisition, Tracking, and Pointing functions in an effort to obtain an understanding of the discrete components and how each component affects the overall system performance. The integrated system is based on the JPL patented Optical Communications Demonstrator Architecture [1]. The architecture contains a Fine Steering Mechanism, Focal Plane Array Detector, Tracking Processor & Control Electronics, Host Processor for User interfacing and control and two Helium Neon visible lasers. The test bed enables the development of the fine pointing control subsystem for Free Space Optical Communications. The work presented demonstrates improvement in the rejection bandwidth of the fine pointing control system from the previous 60 Hz to 75 Hz.

Section 2 defines and describes the existing requirements for fine Pointing Control. Section 3 describes the components of the Acquisition Tracking and Pointing (ATP) test bed. Section 4 describes experiments performed using the test bed. Section 5 discusses results of the experiments. The paper concludes with a summary and approach for future work to achieve less than 1 micro-radian pointing.

2.0 Definition and Requirements of Fine Pointing Control

In this paper, Fine Pointing Control is defined to be the process required to track a reference "Beacon" laser with a tracking laser on a Focal Plane Array Detector. The pointing requirements are driven by the allocated margin to handle mis-pointing. Mis-pointing will cause pointing fades at the receiving station. The major factors contributing to mis-pointing are platform vibrations (S/C), the noise of the sensors (NEA), and the spatial quantization (discretization). This paper will focus on improving the vibration rejection bandwidth in order to compensate for S/C vibrations. Improvement is accomplished by upgrading the legacy Fine Steering Mirror (FSM) with new fine steering mirrors with better open loop bandwidth characteristics.

3.0 ATP Test Bed Architecture

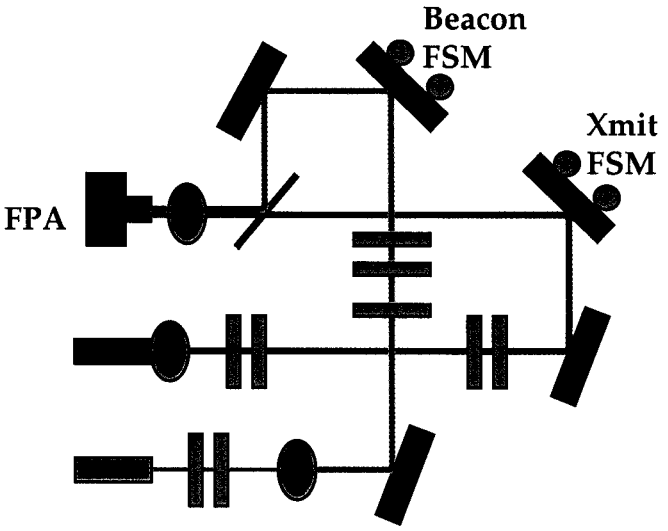

Figure 1 ATP Testbed Optical Setup.

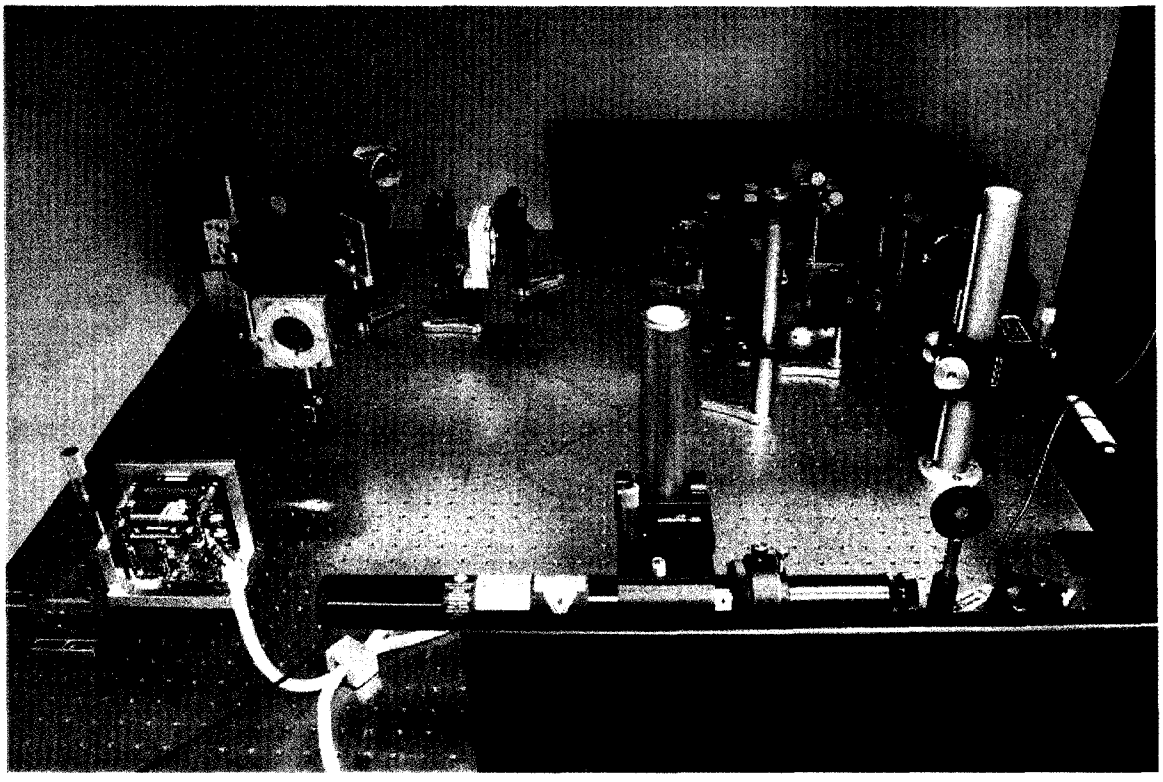

Figure 2 Photograph of the Acquisition, Tracking, and Pointing Test Bed.

3.1 Optical Setup - Gerry Ortiz

The acquisition, tracking and pointing test bed is comprised of four optical channels. These are the transmit beam channel, the beacon channel, the focal plane array (FPA) channel and a public demo channel. This optical layout is based on the Optical Communication Demonstrator single FPA ATP architecture [1]. The transmit channel contains the down link laser beam (simulated here with a red HeNe), which is pointed towards the ground receiver with the fine-steering mirror. Part of the transmit signal is split in a beam splitter and imaged onto the FPA using the optics in the FPA channel. The beacon channel collects the ground laser beacon (simulated here with a green HeNe). This channel also contains a steering mirror for simulating orbital motion, and ground beacon jitter. The beacon channel is combined with the transmit channel using a beam splitter in order to image it onto the FPA. Both beacon and transmit channels are projected onto a target using the public demo channel. This channel allows for ease of visualization of bean motion on the FPA.

As a test bed this setup was designed with certain control parameters to enable characterization of the different components that comprise the ATP system. The system allows control of the spot sizes on the FPA, varying from 130 μm to 60 μm. Also, neutral density (ND) filters have been included to control the intensity of the spots on the FPA. The ND filters enable testing of centroid algorithms and characterization of FPAs. The optical setup includes alignment mirrors that facilitate the ability to replace existing components with upgrade components for the purpose of characterization (eg. replacing the FSM or FPA).

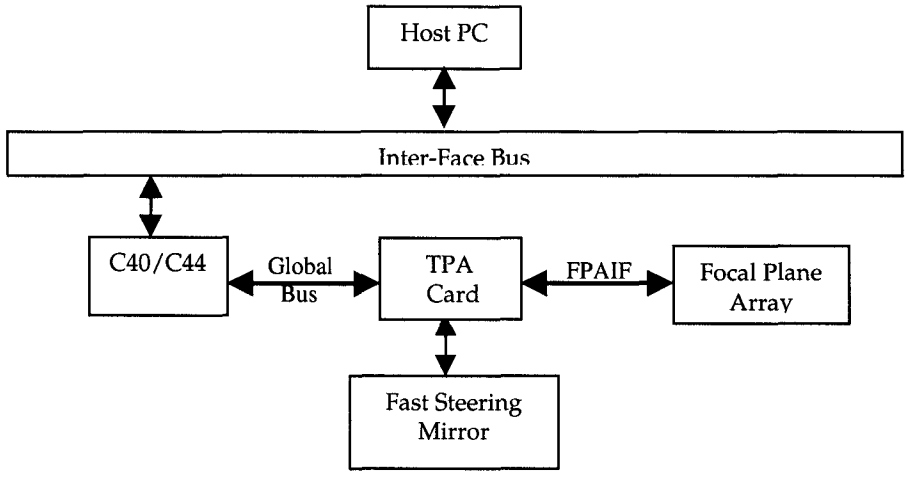

Figure 3 Hardware Description

3.2 Hardware

The tracking system hardware consists of a Host PC, a Texas Instruments TMS320C40 Digital Signal Processor (C40), Tracking Processor Electronics, a modified Dalsa CCD, and Left Hand Designs Fast Steering Mirror (FSM), henceforth denoted as Models FO35 and 15. The C40 implements real-time control of the FSM. The Host PC utilizes a Graphical User Interface to enable user input and data gathering during real-time operation. Communication between the C40 and the Host PC is accomplished via an ISA standard interface to pass data and control parameters from the Host PC to the C40 [2]. The Focal Plane Array implemented is a Dalsa CCD Camera that has been modified to facilitate the extraction of sub-windowed images at high frames, minimum 1000 frames per second for these experiments. The Fast Steering Mirrors are manufactured by the Left Hand Design Corporation.

3.2.1 Modified Dalsa CCD

The Focal Plane Array (FPA) is a modified CA-D1 8-bit, single output Dalsa CCD frame transfer camera. The CCD sensor contains 128x128, 16umx16um pixels with a 16 MHz pixel output rate. The camera has been modified to facilitate fast sub-window readout and has been programmed to extract two 10x10-pixel windows. The Two sub-windows, containing the imaged laser spots of the beacon and transmit laser are read out of the camera at 1000 frames/second in order to optically close the fine pointing control loop via software control. The limit of the frame rate is set by the speed of execution of the tracking software, which is discussed in the experimental section of this document. The location of the sub-windows may fall anywhere within the 128x128-pixel area, resulting in a variable time delay to extract the windowed regions of interest. The time required to obtain the windowed regions of interest is dependent on the size and location of the sub-windows. The time to read a particular sub-window(s) is defined by three time periods that are summed to get the time required for the window read time: Scroll Time, Frame Transfer Time, and Window Row Read Time.

3.2.2 Fast Steering Mirrors

Two fine steering mirrors were characterized and integrated into the ATP test bed to improve on the legacy General Scanning fast steering mirror [2]. The FO-35 & FO-15 FSMs are two-axis reaction compensated fine steering mirrors manufactured by Left Hand Design Corporation. The FSMs consist of the mirror mechanism, sensor demodulation electronics, current-reference driver,

and position-reference servo electronics. The two servo axes are controlled independently via two close loop servos: current-reference and position reference servos. The position servos can operate in one of two modes: base-reference pointing or optical reference pointing. The pointing mode used for fine pointing control is built-in base-referenced position sensor as the feedback sensor [3].

3.3 Real-time Software Implementation

The C40 runs the acquisition, tracking, and fine pointing control software. The algorithms implemented assume the following:

1. There will always be a constant signal for both the Beacon reference signal an the Transmit laser control signal
2. Neither spot shall fall off the field of view of the focal plane array
3. Sub-window overlap of the laser spots will not occur.
4. Initial angular rate of the beacon is minimal.

The assumptions listed above are valid for laboratory operation of the Optical Tracking System.

The acquisition algorithm implemented extracts a single 10x10-pixel window, one full frame per window, from the Focal Plane array in search of a valid beacon centroid signal. The search is implemented by partitioning the 128x128-pixel area into 10x10 sub-windows. A centroid calculation is performed on each sub-window. The centroid algorithm estimates the position of the beacon and reports the result only if a valid beacon signal has been located. A valid beacon signal is defined as a sub-window that contains sufficient intensity based on a predefined value, or intensity threshold, of the sub-window pixel values. The acquisition sequence is completed when all possible sub-windows are processed, recording the window location with the highest intensity value. If the acquisition algorithm locates a valid beacon the software then switches to tracking mode, else the process is repeated until a valid beacon signal has been located. During this time the transmit laser spot is placed in a designated area of the Focal Plane Array so as to avoid confusion between the two laser spots.

Once a valid beacon has been located, the tracking software commences to close the control loop of the steering mirror based on the centroid data, see figure 4. A software state machine executes the transition from acquisition mode to tracking mode. The FSM control loop is optically closed by comparing the beacon position with the transmit laser position with an optical offset added to avoid overlap between the two laser spots. The difference between the two laser spot locations is then used as the error signal into the control loop. The amount of error signal injected into the control loop is initially limited due to the inability of the image tracking software to track laser spots at high angular rates. Once the error signal is at a low level, the full error is then injected into the control loop. The tracking software then attempts to stabilize the line of sight for the transmit laser using optical feedback, as shown if figure 4.

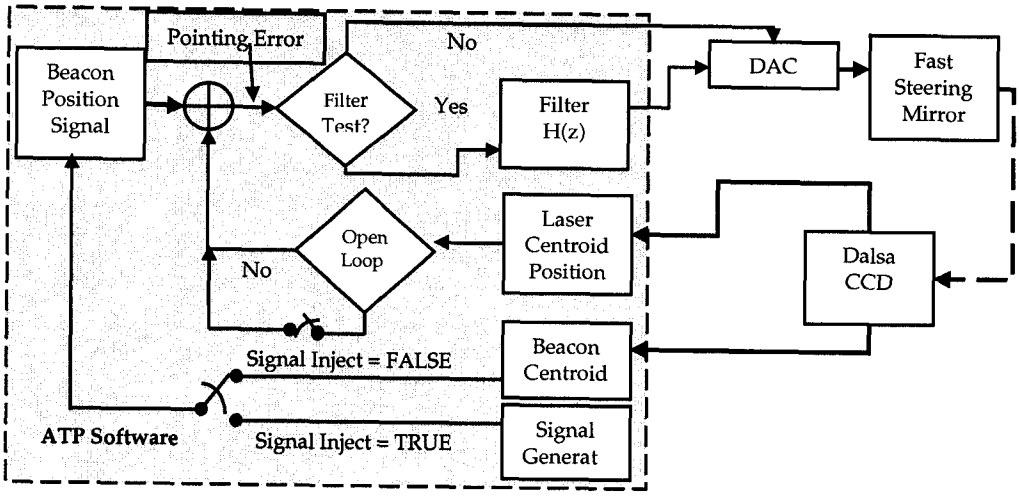

Figure 4 Software Description

3.3.1 Software Timing

The timing of the events that implement the real-time operation of the control loop is critical for optical tracking and pointing control. The amount of time delay induced by digital processing of data used by the feed back path can significantly reduce the performance achievable[4]. Previous experiments demonstrated a 3-sample delay in the optical tracking system digital control loop [2]. The timing of the software versus sample time is shown in figure 5 for three samples of the update loop. The process to update the FSM using optical feedback is a 5-step process:

1. Frame exposure
2. Frame transfer
3. Frame readout
4. Centroid processing
5. Mirror update.

The timing diagram shows the frame exposure, frame transfer, frame readout, frame processing, and FSM control update. At time equal 0, the exposure of frame zero occurs. At time equal 1 the pixel read out, centroid processing and FSM update occurs of exposure zero occurs, while the exposure of frame 1 occurs in the background. At time equal 2 the response of the controller to frame 0 is scene by the Focal Plane Array during the exposure of frame 2, three samples later, while processing of frame 1 occurs. At time equal 3, exposure of frame 3 occurs, and processing of frame 2 occurs, which contains the information of the response of the loop to the very first frame, while other processing occurs as discussed above. Therefore, optical feedback with this type of architecture will have an inherent 3-sample delay.

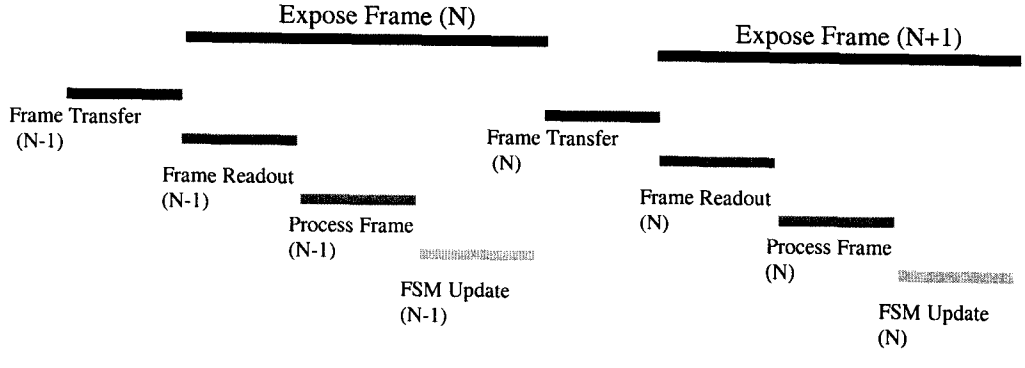

Figure 5 Frame Processing

The software acting in concert with the hardware discussed above is then used to perform experiments for calibration and analysis of the open loop behavior of the fine pointing control system. A digital controller is then designed for the close loop operation of the system.

4.0 Laboratory Measurements

The DAC, FSM servo, and mirror are treated as the system plant for the purposes of analyzing the mirror control system. The majority of the system delay comes from the CCD, which acts as the feedback path. Other system components also contribute to the system delay. The C4x and the C4x software make up the digital filter.

4.1 Software Execution Speed

The software was first benchmarked to determine the maximum update rate possible. The steps described to update the optical control loop in section 3.3.1 were independently benchmarked. The sum of all the processing steps defines the total time required to perform one update of the digital control loop using optical feedback. The maximum possible frame rate was measured to be approximately 1400 frames per second. The frame rate was selected to be 1000 frames per second due to timing variances in the imaging readout. The frame rate selected is a reduction of two from the previous frame rate implemented on OCD [5]. The readout and centroid processing of the pixel data for each sub-window consumes nearly seventy percent of processing time. The centroid algorithm implemented improves the legacy algorithm by enabling estimation of the value of the background offset from the target laser spots. The readout time is twice as slow, compared to the legacy system The legacy system would perform both pixel readout and centroid in one step while the new centroid algorithm splits the operation into two steps.

Table 1 Software Benchmark

Process Step	Time (S)
Frame Readout	294.3×10^{-6}
Process Frame	362.8×10^{-6}
Mirror Update	31.5×10^{-6}
Total	688.9×10^{-6}

4.2 Calibration

After selecting a frame rate, the FPA and FSM misalignments and scaling were characterized and corrected for in the ATP software. The FSM to FPA misalignments and scaling were determined by scanning the FSM in each direction independently while consecutively logging centroid values for 5000 data points at discrete steps across the FPA field of view. The mean value of the centroid data was determined and plotted for each discrete step. A linear fit was then performed on the data to find the transformation to correct for the misalignment and scaling.

4.3 Open Loop Characterization

Once the frame rate was selected, i.e. the system sample rate, and the calibration of the FSM to FPA coordinate was completed, tests were performed to characterize the open loop response of the FSM using the ATP software. The ATP software supports open and close loop characterization of the FSM. The procedure to perform open loop characterization is well-documented [2]. Open loop testing was done by injecting a white noise signal with a five pixel peak-to-peak amplitude. The transfer function that includes the digital controller, FSM, FPA, and software delay was then measured. A linear sub-space [6] digital model was then fitted to the data using the System Identification Toolbox from Matlab. The Matlab derived model and the empirical estimate for both the horizontal and the vertical axes are shown in figures 4 & 5 for the FO-15 and figures 12 & 13 for the FO-35 respectively. The digital models for each axes, shown in Table 2, where a given model is defined as digitally using the z-transform as:

$$M(z) = \frac{\sum_i a_i z^i}{\sum_j b_j z^j}, i = 0,1,...n;\ j = 0,1,...n \quad (1)$$

Table 2 Digital Models

FO-15				FO-35			
Horizontal Axis		Vertical Axis		Horizontal Axis		Vertical Axis	
a_i	b_i	a_i	b_i	a_i	b_i	a_i	b_i
-0.4418	-0.02275	-0.3704	0.01512	-0.3388	0.01386	-0.306	0.01717
0.3822	-0.08699	0.2288	-0.06355	0.1889	-0.04285	0.1427	-0.1448
0.6433	0.3746	0.629	0.1511	0.7113	0.09865	0.4553	0.568
0.001614	-0.6607	0.007317	-0.623	0.008561	-0.4987	0.004139	-1.129
0.0	1.0	0.0	1.0	0.0	1.0	0.0	1.0

The models have –3db bandwidths for the FO-15 Horizontal 331.5 Hz, Vertical Axis 319.8 Hz, FO-35 Horizontal Axis 335.9 Hz, and Vertical Axis 251.5 Hz. Based on the models, closing the feedback loop would result in system instability for both axes for each FSM, FO15 & FO35.

4.4 Close Loop Prediction

Closing the tracking loop would result in instability in both axes for each FSM. Using the z-transform model of the control, PID type control controllers were designed to stabilize the FSMs in both axes. The digital version of the Ziegler-Nichols method for PID control design was used to generate the coefficients [7], with the derivative gain set to zero for the FO-15 due to instability issues. The resulting controllers were implemented as IIR digital filters in the software, figures 6 & 7 FO-15 and figures 14 & 15 FO-35. The close loop performance was predicted using a Matlab simulation by closing the loop, figures 8 & 9 FO-15 and figures 16 & 17 FO-35. The coefficients for each FSM digital controller are listed Table 3.

Table 3 Digital Controllers

FO-15				FO-35			
Horizontal Axis		Vertical Axis		Horizontal Axis		Vertical Axis	
a_i	b_i	a_i	b_i	a_i	b_i	a_i	b_i
-0.05005	-1.0	- 0.1348	-1.0	0.1	0.0	0.25	0.0
0.35	1.0	0.465	1.0	- 0.33	-1.0	- 0.609	-1.0
0.0	0.0	0.0	0.0	0.61	1.0	0.719	1.0

The FO-15 controllers listed above have the following stability margins and predicted –3dB close loop bandwidths.
Horizontal Stability Margins: 4.9 dB, 70.1^0 ; BW = 196.7 Hz
Vertical Axis Stability Margins: 5.7 dB, 62.4^0 , BW = 189.9 Hz

The FO-35 controllers listed above have the following stability margins and predicted –3dB close loop bandwidths.
Horizontal Stability Margins: 5.7 dB, 62.5^0, BW = 229.5 Hz
Vertical Axis Stability Margins: 5.7dB, 61.1^0, BW = 205.6 Hz

4.5 Close Loop Verification

Close loop performance was verified by injecting digital sine waves at discrete frequencies into the control loop. The data was processed to determine the close loop response of each mirrors' axis. During testing, only one axis was tested at a time. The results are shown in, figures 8 & 9 FO-15 and figures 16 & 17 FO-35.

The rejection bandwidth was predicted using Matlab[2,5]. The rejection bandwidth was verified and found to be approximately 60-70 Hz for each FO-15 axis and approximately 70 Hz for each FO-35 axis. The plots are shown in figures 10, 11, 18 & 19, for each mirror respectively.

Conclusion

In conclusion the close loop and rejection bandwidth have been improved from previous experiments using new FSMs. The improvements are apparent even after reducing the control loop sample rate. Time delay limitations in the digital control loop have been identified to be due to the limited processing bandwidth that is characteristic to the implemented hardware and software architecture

Future Work

The next steps to improve the implemented tracking loop are to upgrade the FPA with a larger and faster CCD sensor. We are also looking at implementing inertial assisted beacon tracking concepts to reduce the frame rate of beacon images.

Acknowledgments

This work was carried out by the Jet Propulsion Laboratory, California Institute of Technology, under contract with National Aeronautics and Space Administration. Matlab is a registered trademark of the The Mathworks, Inc.

References

[1] T. Yan, M. Jeganathan, J. R. Lesh, "Progress on the Development of the Optical Communications Demonstrator", *Free Space Laser Communication Technologies IX, SPIE Proceedings*, February 1997.

[2] C. Racho and A. Portillo, "Characterization and Design of Digital Pointing Subsystem for Optical Communications", *Free Space Laser Communication Technologies XI*, Proc. SPIE, Vol. 3615, 1999.

[3] Left Hand Design Corporation, "FSM Operators Manual", *Revision Initial*, September 8, 1998.

[4] B. Lurie, "Feedback limits in the steering mirror loops caused by computer delay", *JPL Memorandum*, September 2000.

[5] M. Jeganathan, et. al., "Lessons Learnt from the Optical Communications Demonstrator", *Free Space Laser Communication Technologies XI*, Proc. SPIE, Vol. 3615, 1999.

[6]P. van Overschee, B. De Moor, "Subspace Identification for Linear Systems: Theory, Implementation, Applications", *Kluwer Academic Publishers*, Norwell, MA1996.

[7] C. L. Philips, H. T. Nagle, "Digital System Control: Analysis and Design", 2nd Edition, *Prentice Hall*, Englewood Cliffs, New Jersey, 1990.

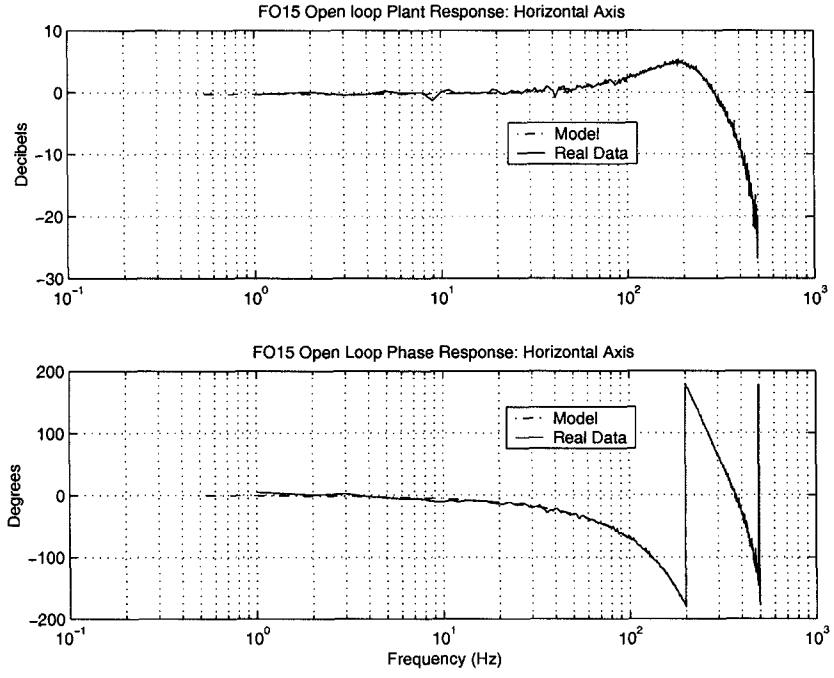

Figure 4 FO15 Open Loop Response – Horizontal Axis

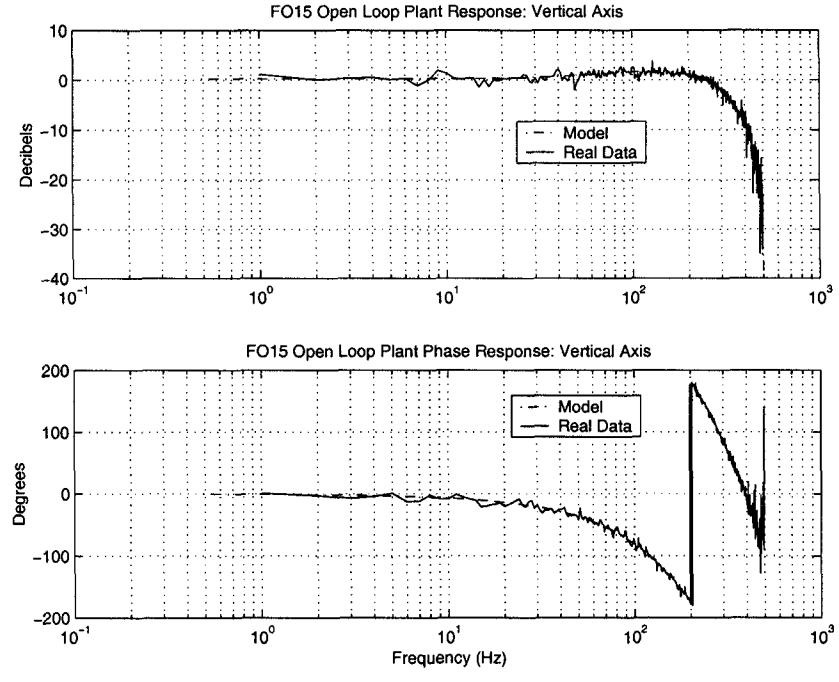

Figure 5 FO15 Open Loop Response – Vertical Axis

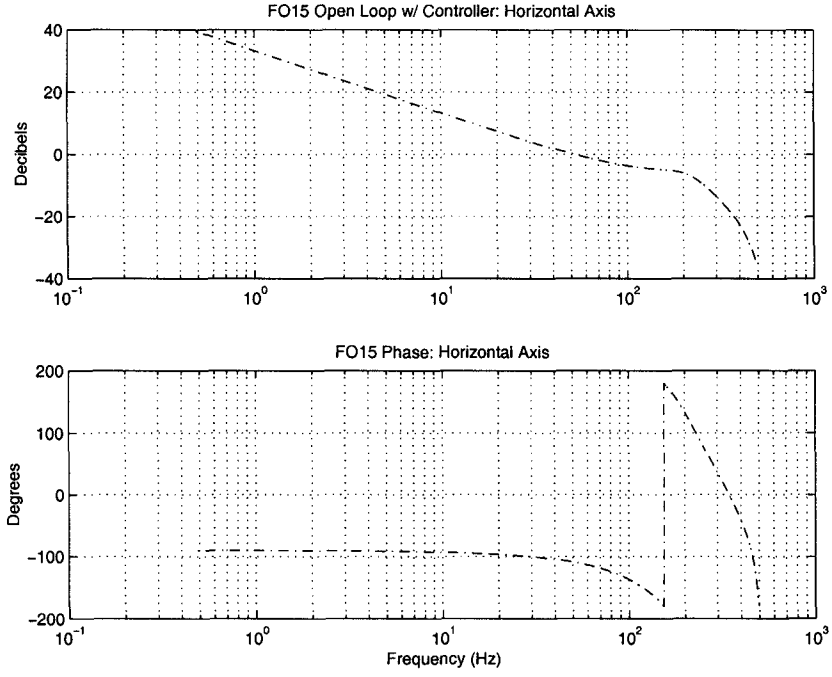

Figure 6: FO15 w/ Controller – Horizontal Axis

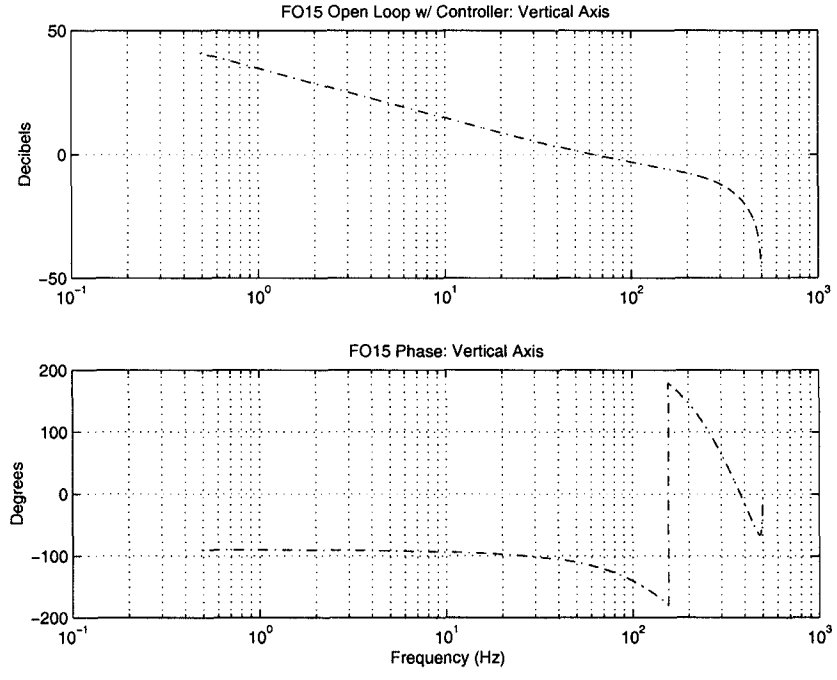

Figure 7 FO15 w/ Controller – Vertical Axis

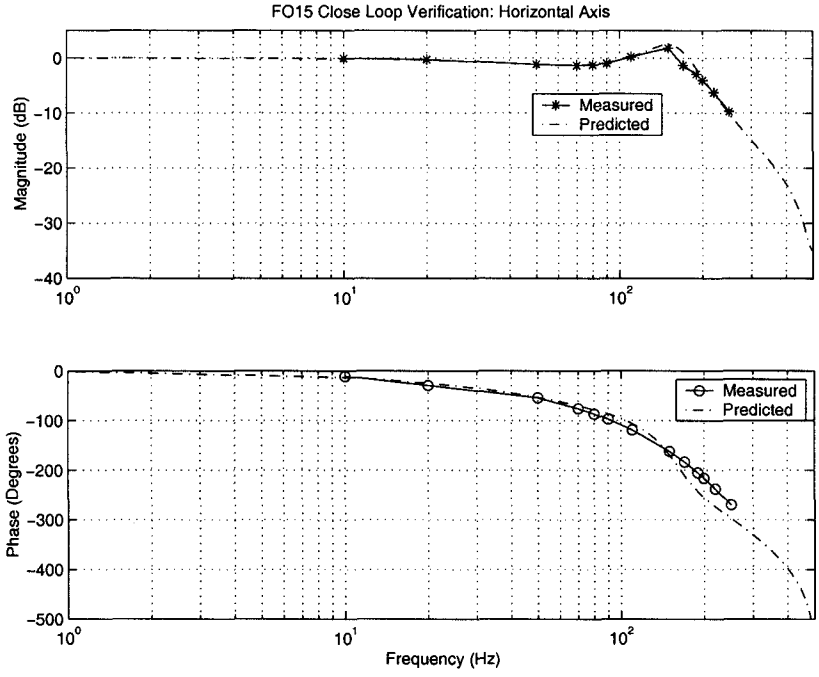

Figure 8 FO15 Close Loop – Horizontal Axis

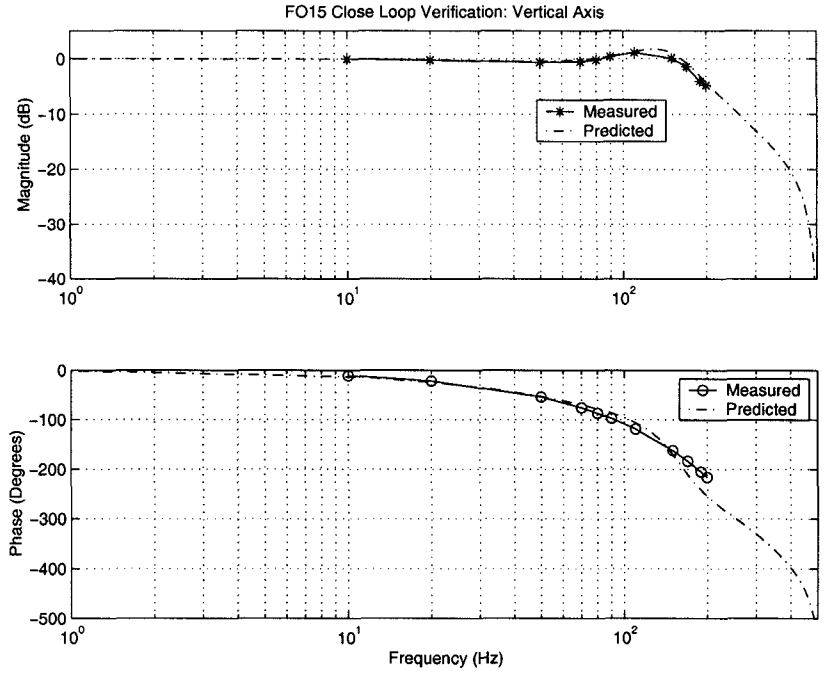

Figure 9 FO15 Close Loop – Vertical Axis

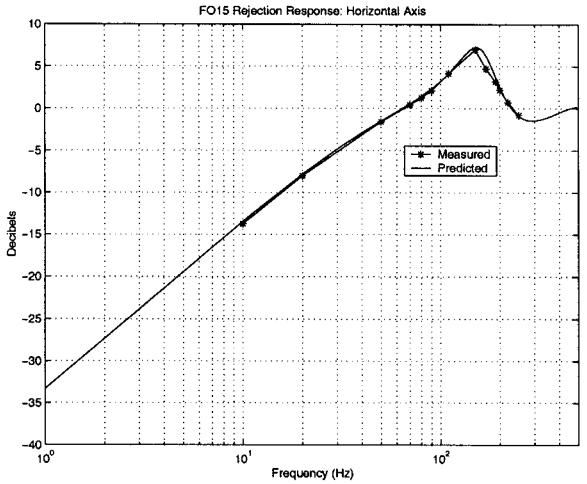

Figure 10 FO15 Rejection Response – Horizontal Axis

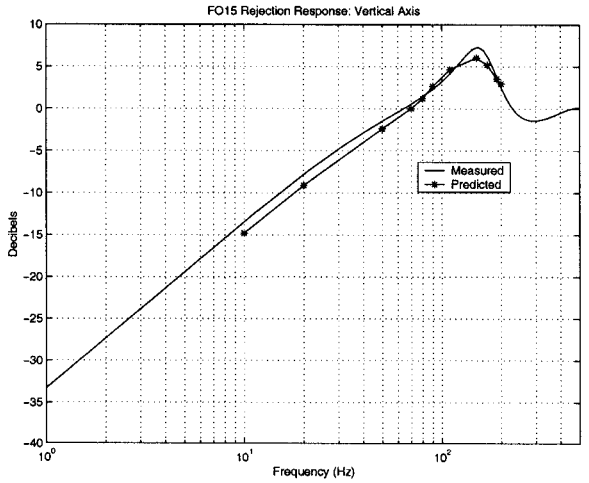

Figure 11 FO15 Rejection Response – Vertical Axis

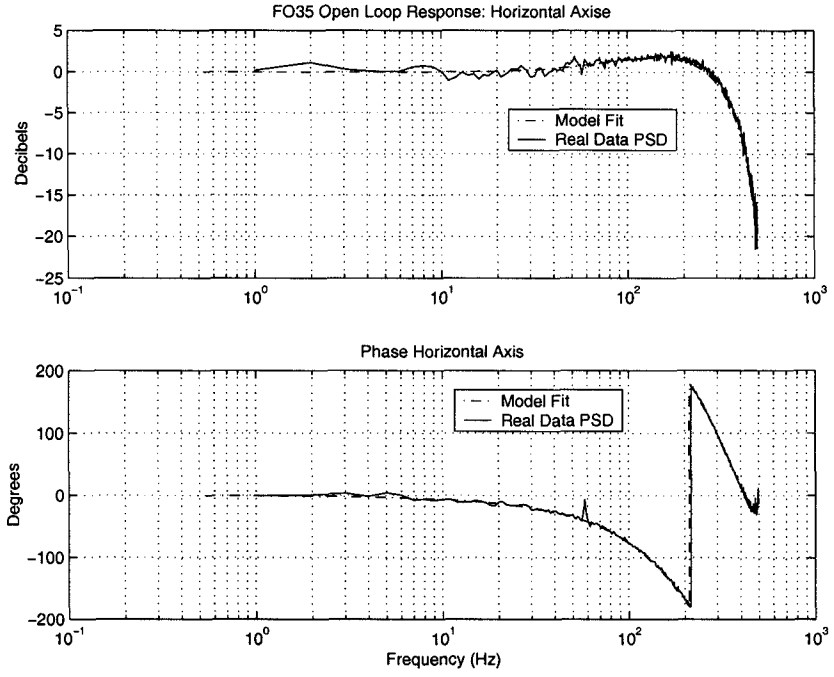

Figure 12 Open Loop Response – Horizontal Axis

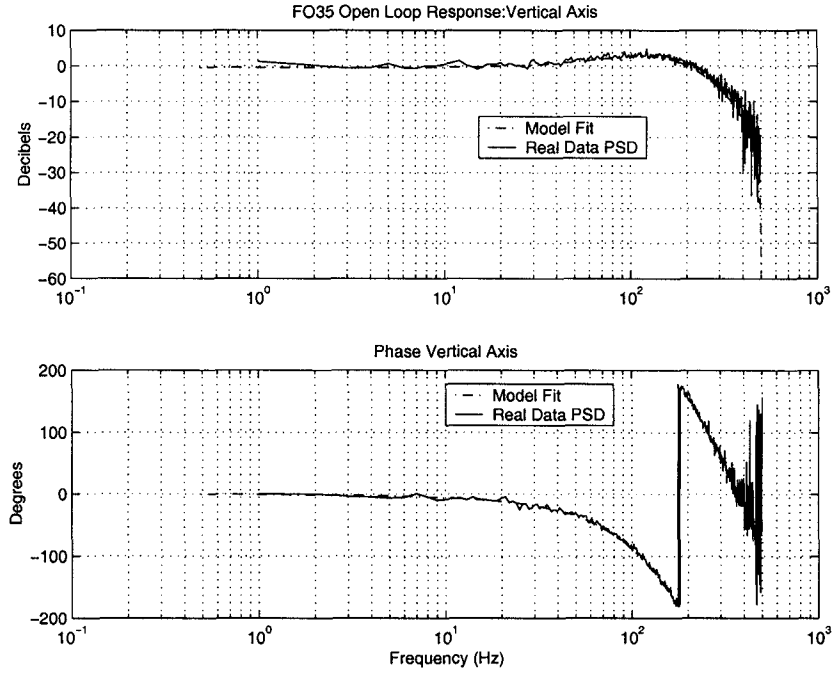

Figure 13 Open Loop Response – Vertical Axis

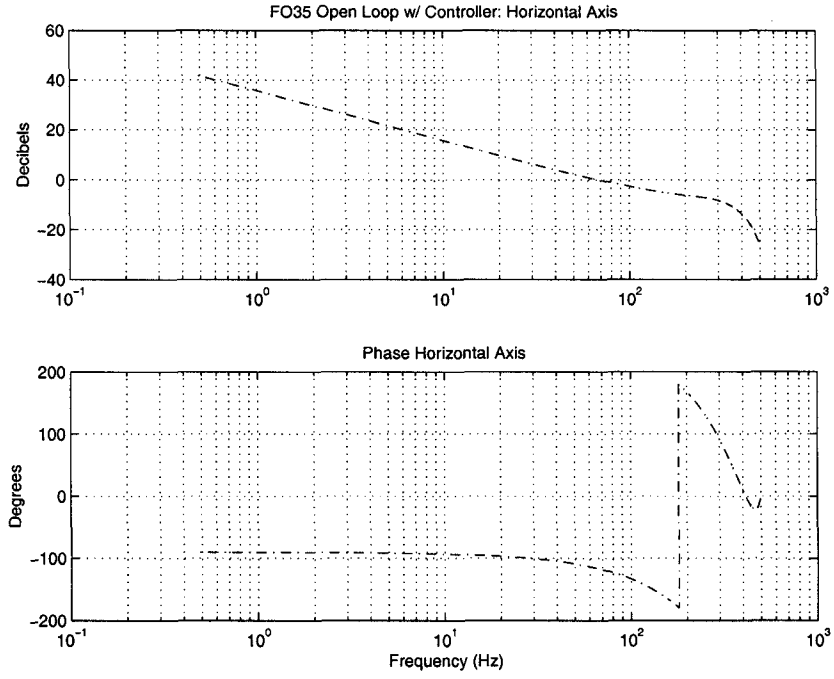

Figure 14 FO35 Open Loop w/ Controller – Horizontal Axis

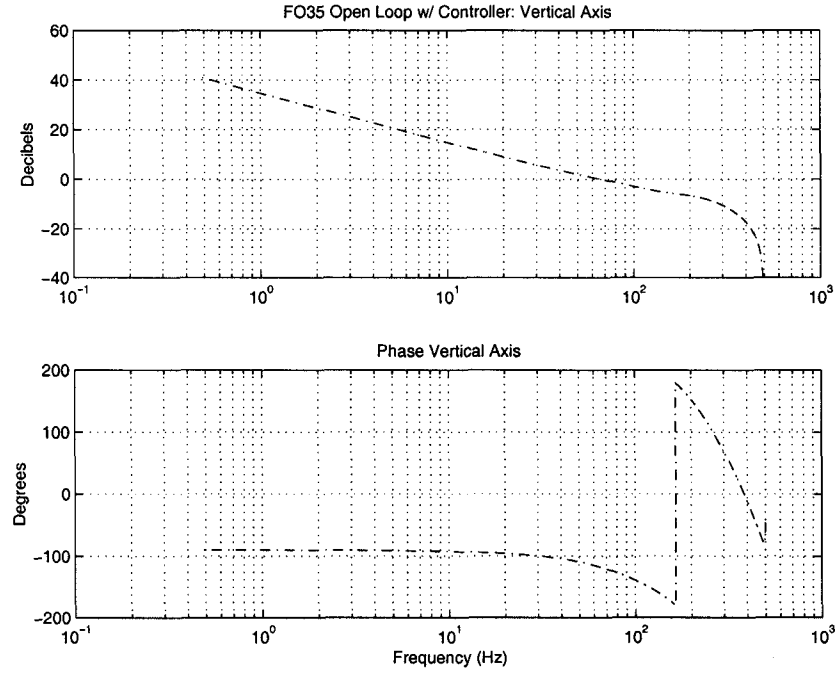

Figure 15 FO35 Open Loop w/ Controller – Vertical Axis

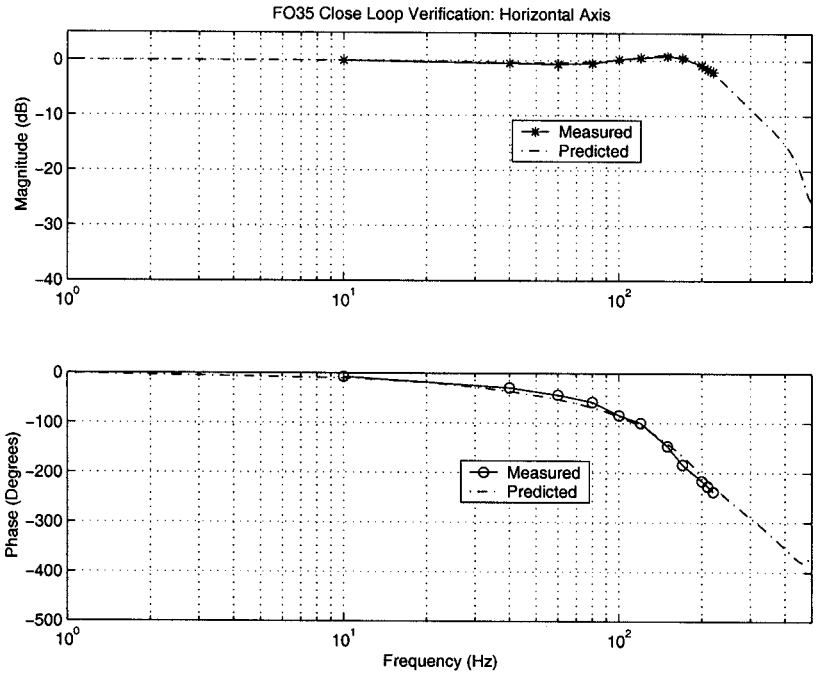

Figure 16 FO35 Close Loop – Horizontal Axis

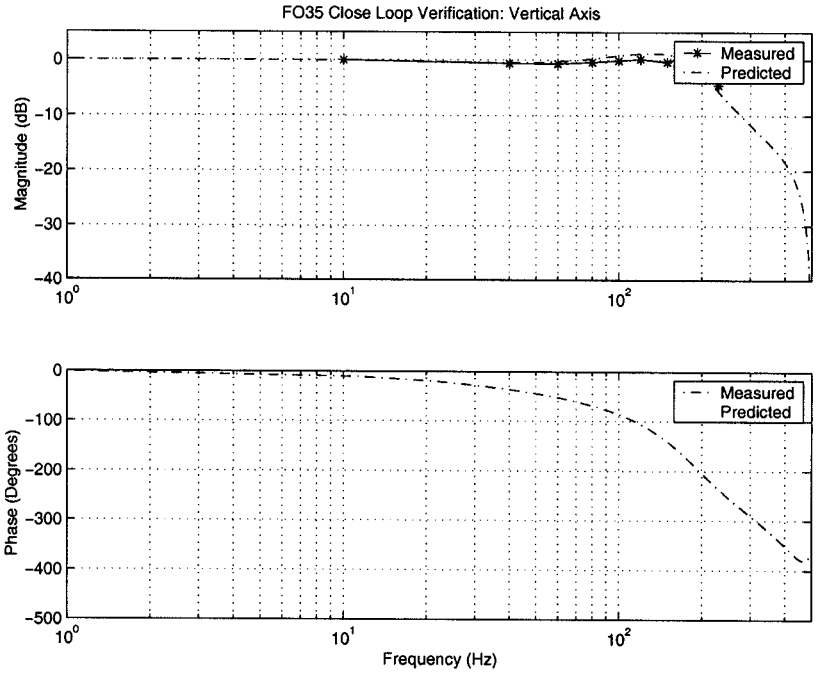

Figure 17 FO35 Close Loop – Vertical Axis

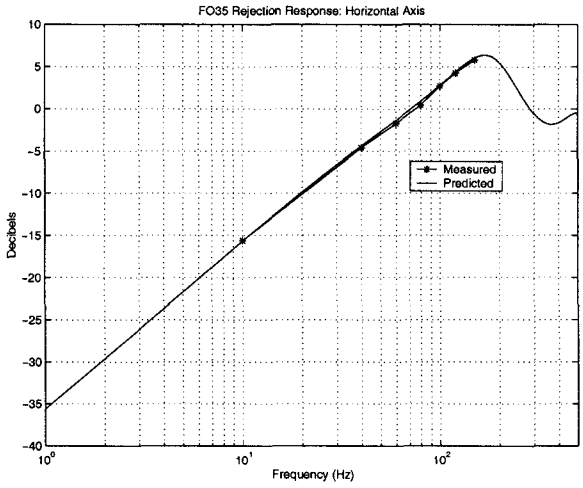

Figure 18 FO35 Rejection Response – Horizontal Axis

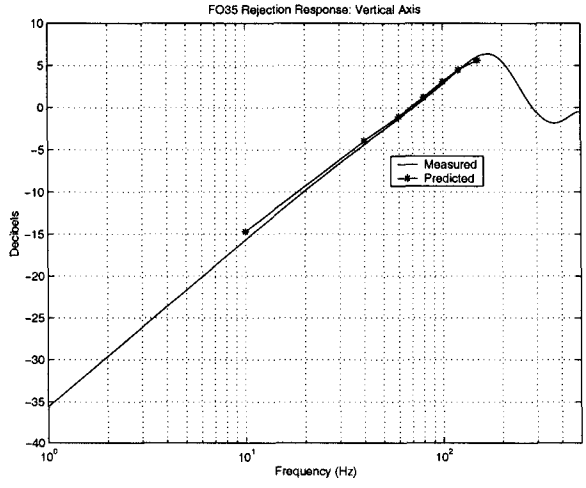

Figure 19 FO35 Rejection Response – Vertical Axis